A VALIDATED TOOL TO PREDICT DRAG PENALTY DUE TO HULL ROUGHNESS DIRECTLY FROM HULL-SCAN DATA.

J.B. Will, I. ’Aliman & B. Nugroho
Department of Mechanical Engineering
University of Melbourne
Parkville, Victoria 3010, Australia
jelle.will@unimelb.edu.au

Henrdiyadi & T. Mulia
PT Samudera Indonesia
Jakarta, Indonesia

F. Taufany
Department of Chemical Engineering
Institut Teknologi Sepuluh Nopember
Surabaya 60111, Indonesia

I. K. Suastika & I.K.A.P. Utama
Department of Naval Architecture
Institut Teknologi Sepuluh Nopember
Surabaya 60111, Indonesia

M. P. Schultz
Department of Mechanical Engineering
Johns Hopkins University
Baltimore, 21218, Maryland, USA

J.P. Monty & N. Hutchins
Department of Mechanical Engineering
University of Melbourne
Parkville, Victoria 3010, Australia
nhu@unimelb.edu.au

ABSTRACT

Field measurements on an operating tanker ship have provided a unique ground-truth measurement of the skin friction drag penalty due to hull roughness. Here, results are presented following 3.3 years of continued operation since cleaning and recoating at dry-dock. At this time, significant biofouling has started to accumulate on the submerged hull and flow measurements of the turbulent boundary layers developing along the flat bottom of the ship reveal a hull-averaged equivalent sand-grain roughness height $k_s = 0.56$ mm and a skin friction drag penalty $\Delta\overline{C_f}|_{L_{wl}} = 55.9\%$ as compared to a hydrodynamically smooth baseline. These data are used to benchmark a methodology for predicting k_s and $\Delta\overline{C_f}|_{L_{wl}}$ directly from in-water hull observations of the surface roughness topology. For this purpose, photogrammetric reconstructions using a hull-surface scanner are combined with a topographical correlation developed for biofouling topographies (’Aliman *et al.*, 2026). This methodology shows promising results, giving an estimated k_s within 21% of the expected value, and a prediction of drag penalty $\Delta\overline{C_f}|_{L_{wl}}$ to within 9% of the benchmark.

INTRODUCTION

The hydrodynamic performance of a ship is closely tied to the roughness state of the submerged hull (Townsin, 2003), with around 50%-90% of the total resistance originating from skin friction for large commercial vessels (Kempf, 1937; Kodama *et al.*, 2000). The detrimental effects from (increased) hull-roughness, specifically due to marine organisms settling on the hull of a ship (biofouling), are well known in the marine industry (Woods Hole Oceanographic Institution, 1952). Hull-roughness comes at a significant price in terms of fuel consumption and environmental impact; the shipping industry is responsible for 3%-4% of global green-house gas emissions (European Maritime Safety Agency, 2021). As such, governing bodies and the shipping industry are strongly incentivised to reduce roughness accumulation during the mandated five-year cleaning cycle of a mercantile vessel. This battle against marine growth has led to the widespread adoption of various types of antifouling coatings systems, but in the long run these coatings lose effectiveness and marine growth inevitably begins to colonise the ship’s hull. In more extreme cases, this biofouling almost doubles the drag (Schultz *et al.*, 2011). Currently, however, there is a lack of reliable predictive tools that can estimate this biofouling-induced drag penalty directly from hull observations. This limitation, in large part, stems from current correlations that aim to predict the equivalent sand-grain roughness height k_s from topography not being trained on the types of surfaces relevant to fouled ship hulls. This inability to prescribe a cost to hull roughness limits the ability to make informed decisions. For example, it is impossible to perform a meaningful cost-benefit analysis of a particular strategy aimed at maintaining hull condition (e.g., more frequent dry-docking, better coating technologies, in-water cleaning, etc.). This work aims to address these issues by testing a correlation that predicts k_s (and hence the total skin friction penalty; $\Delta\overline{C_f}|_{L_{wl}}$) based on topographical inputs provided by dive inspections. The resulting predictions can be validated against actual drag penalty measurements obtained on the operating ship using through-hull measurements of the turbulent boundary layers formed over the hull.

FIELD MEASUREMENTS

The data presented in this work are part of a longitudinal research campaign investigating the roughness state and

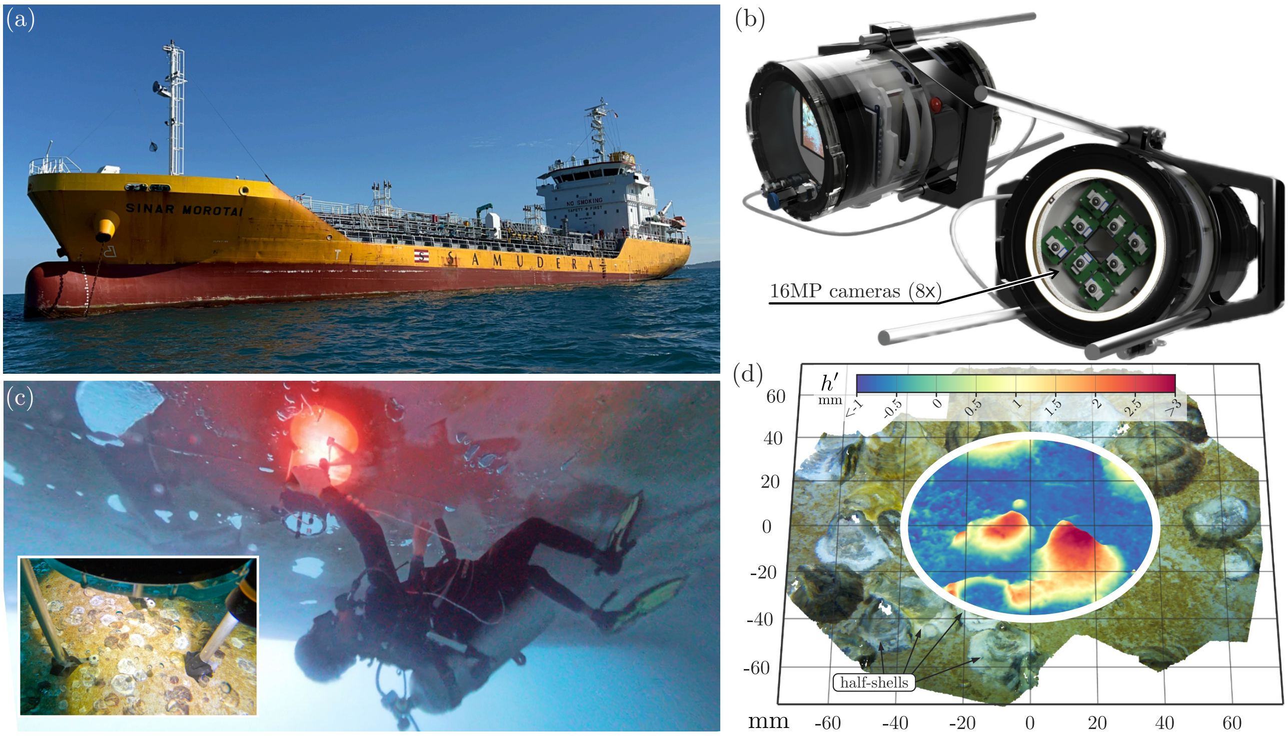

Figure 1. (a) MT Sinar Morotai at anchor before a dive-inspection. (b) AQUAMARS, a diver-operated in-water roughness inspection platform developed at the University of Melbourne. Eight 16-megapixel cameras image the same field of view from various angles, allowing for photogrammetric reconstruction of the surface. (c) A diver operating AQUAMARS underneath the Sinar Motarai. The inset shows the roughness imaged by AQUAMARS, as seen from a camera mounted on the side of the housing. High-density shell roughness is present at this location on the hull. (d) A real-colour point cloud reconstruction of the area shown in the inset of (c). Within the white circle at the center of the domain a false colour height map of the surface elevation with respect to the mean is shown.

skin friction drag penalty of the chemical tanker Sinar Morotai (see Figure 1a). This vessel, operated by Samudera Indonesia, has a water-line length (L_{wl}) of 92.7 meters, a draft of 5.8 meters (depth of the bottom below the loaded waterline) and a beam (width) of 14.6 meters. The vessel was dry-docked at Semarang shipyard in March 2022, where it was cleaned to an ISO 8501 Sa2 standard, and a self-polishing copolymer (SPC) antifouling coating was applied. At the same time, a marine grade window was installed on the flat underside of the ship, approximately 67.5 meters downstream of the forward perpendicular (FPP) and 0.65 meters off the centreline on the port side of the ship, see Figure 3(a). This window provides optical access to the turbulent boundary layer (TBL) developing along the flat bottom of the ship, allowing wall-normal velocity profiles to be taken using a laser Doppler anemometry (LDA) system mounted inside the double-hull of the ship.

Over the 3.3 years following dry-dock, six measurement campaigns were carried out to monitor the hull state and drag penalty of the vessel. This is accomplished by: 1) Performing dive-inspection documenting the fouling state of the hull – in terms of spatial distribution of fouling and local surface height maps – using underwater cameras and AQUAMARS; an in-house developed photogrammetry system. And 2) by performing flow measurements of the TBL developing over the underside of the ship (as presented in Figure 2) using the LDA. In this work we will discuss the results of the sixth campaign, conducted in July 2025. During this campaign the operating conditions of the ship were as follows: the mean relative velocity between ship and water (the free-stream velocity) was equal to $U_\infty = 5.38\,\mathrm{m\,s^{-1}}$ and the mean kinematic viscosity was determined to be $\nu = 0.838 \times 10^{-6}\,\mathrm{m^2 s^{-1}}$. Furthermore, by assuming outer layer similarity in the measured mean velocity and variance profiles, the friction velocity at the window was calculated to be $U_\tau = 0.185\,\mathrm{m\,s^{-1}}$.

Turbulent boundary layer measurements

For each campaign, multiple wall-normal (z) profiles of the streamwise velocity statistics are obtained using the LDA. From these, the wall-shear stress ($\tau_w = \rho U_\tau^2$, where ρ is the fluid density) is estimated by assuming outer-layer similarity

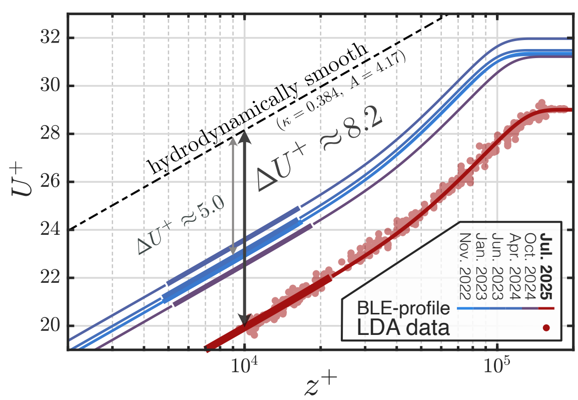

Figure 2. Inner-scaled mean velocity ($U^+ = U/U_\tau$ vs. $z^+ = zU_\tau/\nu$) for the six experimental campaigns on the Sinar Morotai. Hama roughness function (ΔU^+) is indicated for the baseline (blue) and the current (red) hull states with respect to the hydrodynamically smooth logarithmic (black dashed) line.

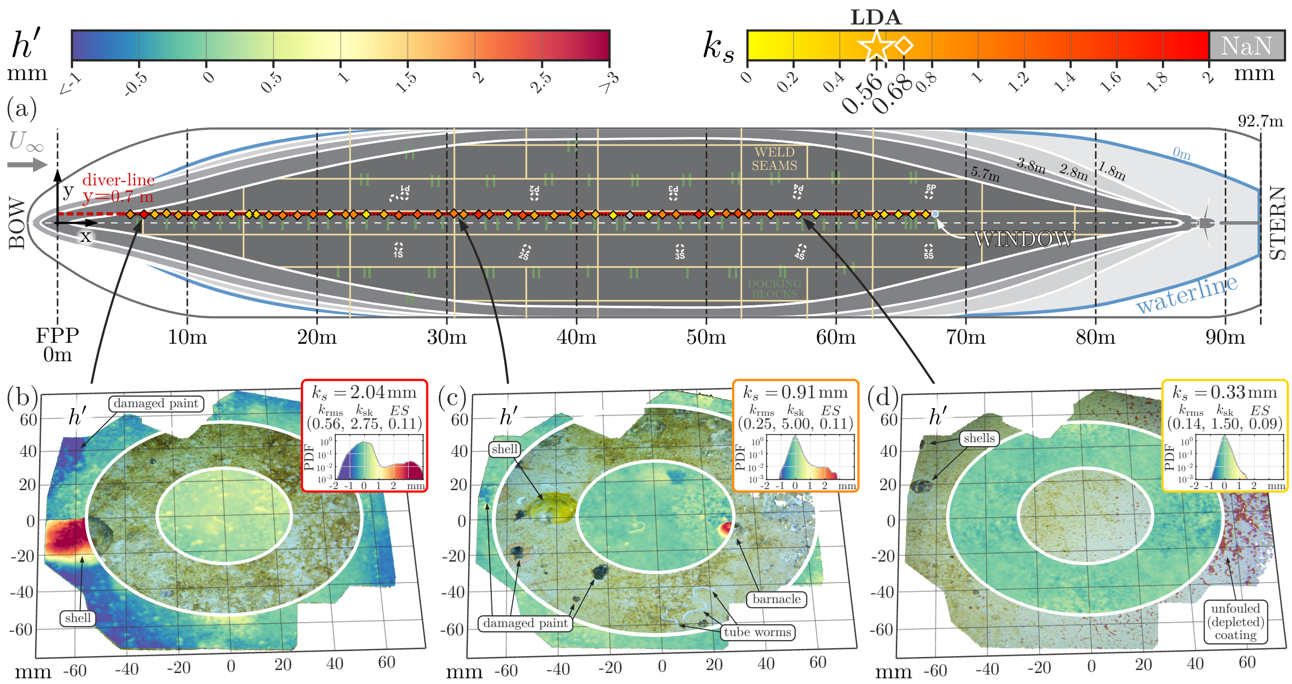

Figure 3. (a) Schematic depicting a bottom-up view of the hull of the Sinar Morotai, the red line indicates the line upstream of the LDA window sampled during the dive-inspection. The markers along this line indicate locations of AQUAMARS scans, with the colour representing the estimated value of k_s. (b–d) Topographical maps for AQUAMARS scans at three locations along the line in front of the LDA window. Real colour point cloud surface reconstructions are presented along with false colour height maps of the meshed and filtered surface data. The inset shows a PDF of the height h' while also listing the predicted value of the equivalent sand-grain roughness height (k_s) from Eq. (1) together with the statistics of the meshed and filtered surface inputted in the roughness correlation.

of the mean velocity (U) and the velocity variance, following the approach by Monty *et al.* (2011). In processing these data, we correct for variations in the relevant fluid properties, density, kinematic viscosity, and refractive index. This is done by using publicly available sea surface temperature and salinity data from satellite observations. In addition, the measured mean and variance of the streamwise velocity are corrected for temporal variations in the free-stream velocity due to changing sea state (e.g. waves and current) and atmospheric (wind) conditions. Composite profiles (Chauhan *et al.*, 2007) best fitting the inner scaled mean velocity LDA data ($U^+ = U/U_\tau$ versus $z^+ = zU_\tau/\nu$, here a superscript '+' indicates inner normalisation i.e. using U_τ and ν) for all six campaigns are shown in Figure 2. For the first four campaigns (blue lines) the downwards shift of the mean profile in the logarithmic region with respect to the smooth wall profile remained constant at $\Delta U^+ \approx 5.0$ to within measurement uncertainty. This downward shift is directly related to the skin friction drag penalty. However, in campaign six, due to an increase in biofouling on the ship's hull, ΔU^+ increased to around 8.2, as indicated by the red markers in Figure 2. This measured value of ΔU^+ can be used to estimate k_s^+ at the window location (using the fully rough asymptote). This, in turn, can be used as input for an integral boundary layer evolution method (see Prandtl & Schlichting 1934; Granville 1958; Monty *et al.* 2016) to predict the evolution of a canonical, two-dimensional, zero-pressure gradient, turbulent boundary layer along a flat plate. In this way, the equivalent sand-grain roughness $\overline{k_s} = 0.56$ mm, reflecting the upstream roughness history, can be estimated. This evolution also provides an estimate of the integrated skin friction drag penalty (compared to a hydrodynamically smooth baseline) of the ship's hull, which *for the full water-line length* is found to be $\Delta\overline{C_f}|_{L_{wl}} = 55.9\%$ at the time of campaign 6.

The biofouling time-line

Based on the dive-inspections, performed before each LDA measurement campaign, examining the submerged hull of the Sinar Morotai, it was determined that during the first two years of operation (campaigns 1–4) the roughness condition of the hull remained relatively unchanged. This observation is consistent with the TBL measurements over the same period presented in Figure 2, which showed no significant change in the value of ΔU^+. At this time, the majority of the submerged hull ($\sim 99\%$), consisting of the regions that had undergone cleaning and where recoated at dry-dock, remained predominantly clean, highlighting the effectiveness of the applied anti-fouling system over this period. Consequently, the main sources of hull roughness at this time were the weld seams and the docking block marks; areas that were not cleaned and recoated since they were obstructed by the wooden sleepers on which the ship was resting in dry-dock. The locations of both features are mapped in Figure 3(a).

By campaign 4 it was observed that large portions of the hull began to show discolouration from the original brown/red to white/grey, see rightmost section of Figure 3(d). This is most likely caused by the grey anti-corrosion undercoat becoming exposed through wear or due to gradual depletion of the active components from the SPC coating. In either case, this discolouration is indicative of reduced protection against marine growth. For campaign 5, in October 2024, the regions that previously showed the most (white/grey) discoloration were beginning to foul, turning green/brown and accumulating sparse tube worms, shells, and barnacles coverage. These patches of roughness were concentrated between 15 and 50 meters downstream of the FPP. At this time, the roughness state of the hull was patchy and heterogeneous.

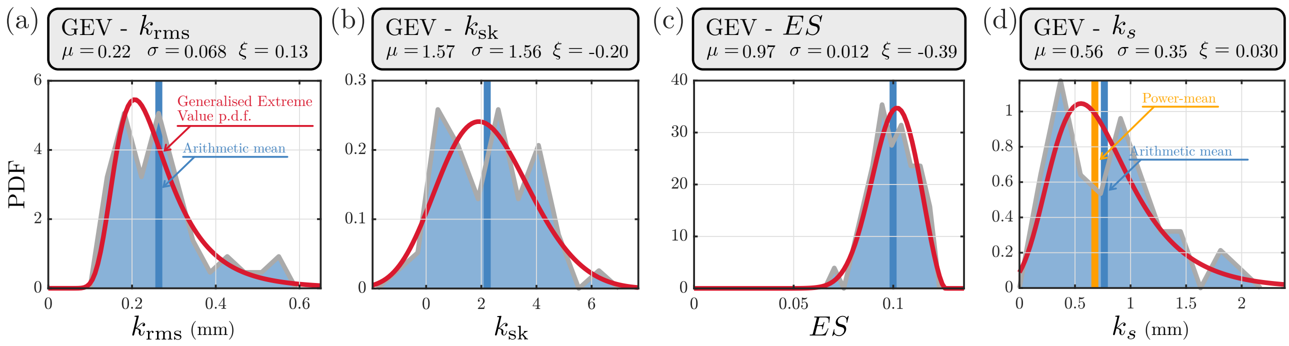

Figure 4. Probability Density Functions (PDF) of the observed values of (a) k_{rms}, (b) k_{sk}, (c) ES, and (d) the predicted values of k_s, for the 53 scans measured upstream of the LDA window on the Sinar Morotai. The blue area shows the distribution of observed values and the red line a Generalized Extreme Values (GEV) PDF based on the observations; giving a practically usable distribution of realistic biofouling encountered in the field. The vertical blue lines shows the arithmetic mean of the respective distributions and the yellow line the power-mean of k_s.

Current hull-roughness observations

The present work details the hull roughness characterisation of the Sinar Morotai during campaign 6 using a custom-built 3D underwater surface scanner AQUAMARS (Kevin *et al.*, 2025), depicted in Figure 1(b) and shown in operation under the Sinar Morotai in Figure 1(c). Three-dimensional data for the scanned area is obtained via photogrammetric reconstruction of eight images captured by eight individual 16-megapixel cameras with the same field of view seen from different viewing angles. The photogrammetry step is performed by the commercial software *Agisoft Metashape*. A lens correction for each camera is performed to account for distortion due to both the camera lens and the air-water interface of the scanner body. Reconstruction generates a *point cloud* data set with a near homogeneous density of approximately 200 points per mm^2 or around 3.2×10^6 points per scan in total. The reconstructed area is approximately $0.016\,\mathrm{m}^2$. Two targets, visible in Figure 1(c), connected to the legs of AQUAMARS are in constant view. The distance between these two targets is known to within 1 mm and is used to convert the point cloud data into physical dimensions. An example of a reconstruction is shown in Figure 1(d) in mixed real and false colour; with the colour map representing the surface height $h'(x,y) = h(x,y) - \langle h \rangle$, where $\langle \cdot \rangle$ indicates a planar average. These reconstructions are highly spatially resolved with well-converged statistics of the imaged surface area. Furthermore, the data are obtained less than 24 hours before the start of the flow measurements and are therefore considered to accurately capture the hull state at the time of the LDA measurements.

While point cloud data can be used directly to calculate the statistical moments of h'; k_{rms} (root mean square) and k_{sk} (skewness), obtaining the effective slope, defined as $ES = \langle |\mathrm{d}h'/\mathrm{d}x| \rangle$, requires an additional step. Here, we bin the data to a regular mesh with a $0.1 \times 0.1\,\mathrm{mm}^2$ resolution. 2D Gaussian filtering with a standard deviation of 0.3 mm is performed to reduce the small wavelength noise present in the data; this filtering value was determined *a priori* by testing the effect of different filtering length-scales on the value of ES, with the goal being to remove the point cloud noise while preserving the roughness features. This meshing and filtering most certainly introduces a degree of arbitrariness, but without any filtering, the noise in the data would corrupt the gradient calculation necessary to compute ES. All parameters presented in this work are calculated based on the meshed and filtered height maps.

The dive-inspection revealed that the previously observed degradation of the SPC coating had resulted in an almost complete coverage of marine growth; the majority of the hull is covered in a brown/yellow/green layer as illustrated in the example scans in Figure 3(b–d). In total 53 height maps were obtained along the line upstream of the window (red line and diamond markers in Figure 3a) and only one of these scans was partially free of fouling (shown in Figure 3d). This observation is corroborated by the video footage from the second diver using a 360° camera. Hard fouling was most prevalent between 15 and 50 meters downstream of the FPP, the same region where the first signs of fouling were noted in the previous inspection. The three topographies in Figure 3(b–d) are examples of three levels of fouling encountered from rough to smooth. Shown alongside the topography maps in Figure 3(b–d) are the probability density functions (PDF) of $h'(x,y)$ as well the statistical quantities k_{rms}, k_{sk} and ES. In Figure 3(b,c) large flat shells are visible, which are the dominant type of fouling observed for this inspection. As can be seen in Figure 3(b), this type of roughness results in a PDF of h' that is multi-modal since the flat top of the shells results in a second peak. This effect is even more prominent for denser shell coverage as in Figure 1(d), which was obtained at a different location on the hull and shows some of the worst observed fouling. Figure 3(c) shows a heavily skewed distribution which is primarily due to the sole barnacle captured in all of the scans upstream of the LDA window. This scan also exhibits paint damage and tube worms (both were commonly observed across all scans) broadening both sides of the PDF and increasing k_{rms}. Finally, Figure 3(d) shows a relatively smooth topography with lower k_{rms} obtained in the area just upstream of the LDA window. The distribution is positively skewed due to the presence of small shells. The PDFs of k_{rms}, k_{sk}, and ES for all 53 scans are included in Figure 4(a–c), a Generalized Extreme Value (GEV) PDF fit to the data is included for each parameter, providing a usable statistical description of the roughness on the Sinar Morotai. These distributions show a skewed distribution of k_{rms} with large positive outliers, a broad near-Gaussian distribution of k_{sk}, and a surprisingly narrow distribution of ES, with the maximum value not exceeding 0.15. Note that the low ES is not due to over-filtering of the surface data but a feature of the observed type of biofouling roughness with more shells and less barnacles.

VALIDATING FULL-SCALE DRAG PREDICTION

The objective of this work is to use the 53 surface topographies, representing the upstream roughness history, to estimate the roughness-induced skin friction penalty and compare this to the flow measurements at the window location. In this work, we focus on the roughness-correlation approach, which expresses k_s in terms of statistical surface properties. The functional form that we will be testing is pioneered by Forooghi *et al.* (2017) and takes into account three statistical properties of the surface topology: 1) a roughness height dimension (k_{rms})[1], 2) a measure for sparseness and asymmetry of the height distribution; (k_{sk}), and finally 3) a measure for steepness; (ES). The correlation takes the form:

$$k_s = k_{\text{rms}} \left(a_2 k_{\text{sk}}^2 + a_1 k_{\text{sk}} + a_0 \right) b \left(1 - e^{-c ES} \right), \qquad (1)$$

and is linear in k_{rms}, quadratic in k_{sk}, and asymptotically exponential in ES. Two versions of the coefficients are presented in Table 1. The first is a fit of Eq. 1 to the original training data, which only spanned a skewness domain of $-0.35 \le k_{\text{sk}} \le 0.68$ and is therefore extrapolating significantly for the type of roughness observed in the field (see Figure 4b). The second set of coefficients was recently developed by fitting the functional form of Forooghi *et al.* (2017) to an expanded training data set covering $-1 \le k_{\text{sk}} \le 5$ (see 'Aliman *et al.* 2026 for full details).

Table 1. Coefficients for the roughness correlation in Eq. (1). Note that, as explained in 'Aliman *et al.* (2026), the original coefficients presented for Forooghi *et al.* (2017) are *refitted* to a wider set of training data and reformulated in terms of k_{rms}, instead of the original peak-to-trough height.

	a_2	a_1	a_0	b	c
Forooghi	-0.052	0.552	0.678	10.8	2.77
current	-0.346	2.82	3.37	2.33	1.82

Examples of the application of the current model are shown for the three topographies in the insets of Figure 3(b–d) showing the input statistics and the calculated value of k_s for each. The extracted values of k_s (and their positions) for all 53 scans are indicated in Figure 3(a) by the colour of the markers with the mapping presented at the top right. The PDF of the k_s values obtained from the 53 scans is shown in Figure 4(d). Note that one of the surface scans resulted in a *NaN* value; this was, in fact, a negative k_s due to large negative skewness (-1.21) beyond the range of the training data. Due to the negative coefficient (a_2), the model can yield negative k_s for small (and very large) skewness. This, of course, is non-physical and reflects a limitation of the fitted functional form.

With this roughness map obtained, each individual scan is treated as a representative sample of the 'local area', with all topographies being weighted equally; each representing ~ 1.2 m of development length or around two times the boundary layer thickness at the window location. This approach assumes that the flow is in equilibrium with the local surface condition at each streamwise station and that the effect of the roughness on the integrated drag is the result of the cumulative effect of all surfaces. Since skin friction is not linear in k_s we can not simply take the arithmetic mean to obtain the hull-averaged equivalent sand-grain roughness height ($\overline{k_s}$), instead a power-mean is used. As suggested by Hutchins *et al.* (2023), we will use a power of 0.25, and for simplicity, we will neglect streamwise weighting of the samples since this effect was found to be of secondary importance Vishwanathan *et al.* (2025). Using the current roughness model, a power-mean averaged value of $\overline{k_s} = 0.68$ mm is obtained. This value is 21% higher than k_s obtained from the LDA measurements on the operating ship. For comparison, the original coefficients suggested by Forooghi et al. (2017), as given in Table 1, would have given a power mean averaged $\overline{k_s}$ that is 75% higher ($\overline{k_s} = 0.98$ mm).

[1] Peak-to-trough roughness height in the original work.

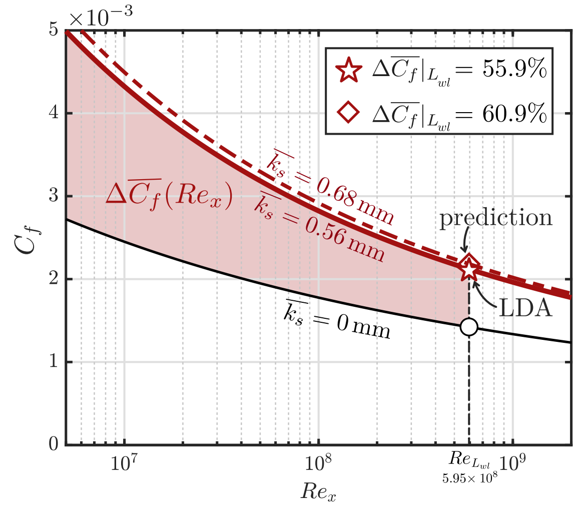

Figure 5. Local skin friction coefficient vs. streamwise Reynolds number for three roughness conditions. (Black line) hydrodynamically smooth $k_s = 0$; (solid red line) $k_s = 0.56$ as obtained from LDA measurements; (dashed red line) $k_s = 0.68$ as predicted based on the dive-inspection data. Area under the curves represents the hull-averaged skin friction $\overline{C_f}$ and the red shaded area denotes the hull-averaged skin friction penalty due to roughness.

Table 2. Results in terms of roughness height and skin friction drag penalty. The first row shows estimates from flow measurements based on the downwards shift of the mean profile in the logarithmic layer of the TBL and the row *predicted* gives a power mean estimate based on the *current* roughness correlation using the AQUAMARS scan data from the dive-inspection .

	k_s (mm)	k_s^+ (-)	$\Delta\overline{C_f}\|_{L_{wl}}$ (%)
flow measurements	0.56	124	55.9
predicted	0.68	150	60.9

In Table 2 the values of $\overline{k_s}$ are shown based on ΔU^+ from the flow measurements using a fully rough assumption and for the predictions based on the dive-inspections. Also included in the table are the roughness Reynolds numbers at the LDA location, indicating that at operational conditions the ship's roughness state is well into the fully rough regime ($k_s^+ > 70$).

Although the calculation of $\overline{k_s}$ from dive-inspection data is of academic interest, the accuracy of the prediction in terms of skin friction drag penalty of the vessel is of more practical relevance. To address this, Figure 5 shows the local skin friction coefficient $C_f = 2\,\tau_w/(\rho\,U_\infty^2)$, as a function of streamwise Reynolds number ($Re_x = U_\infty x/\nu$), with the dashed vertical line indicating the full water line length of the ship. Three roughness cases are shown in the figure, the black solid line indicates $C_f(x)$ for a hydrodynamically smooth wall ($\overline{k_s} = 0$), the solid red line for $\overline{k_s} = 0.56$ mm as per the flow measurements, and the dashed red line for $\overline{k_s} = 0.68$ mm as predicted based on the dive-inspections. The hull averaged skin friction coefficient $\overline{C_f}$ is calculated from the area under the curves. The skin friction drag penalty (red shaded region) expressed as a percentage increase with respect to hydrodynamically smooth is given by $\Delta\overline{C_f} = (\overline{C_f}_r - \overline{C_f}_s)/\overline{C_f}_s$, where $\overline{C_f}_r$ is the rough wall and $\overline{C_f}_s$ the smooth wall hull-averaged skin friction coefficient for the same development length. Table 2 shows the $\Delta\overline{C_f}$ comparison, indicating that the predicted skin friction penalty from the dive-inspection data is within 9 percentile points of the flow-based estimate.

CONCLUSION AND DISCUSSION

In this work, a roughness correlation model developed to work for ship hull roughness is tested using real-world data obtained from field measurements on the chemical tanker Sinar Morotai. The goal of the model is to accurately estimate the skin friction drag penalty based on height maps of the roughness on the bottom of a ship obtained from dive-inspections. Flow measurements of the turbulent boundary layer below an operational tanker ship, obtained using through-hull LDA, provide a benchmark estimate of the hull-averaged $\overline{k_s}$ and the skin-friction penalty $\Delta\overline{C_f}$, which are used to test and validate the predictive methodology. Roughness height maps on the hull of the Sinar Morotai were obtained after three years and four months of continuous ship operation using AQUAMARS, a diver-operated photogrammetry system developed at the University of Melbourne. These showed that the line upstream of the window is completely covered in a layer of algae and other substrate roughness with intermittent hard fouling, primarily flat shells and tube worms. Roughness statistics for 53 locations upstream of the window (~ 67.5 m) were calculated from gridded, filtered point cloud data. The equivalent sand-grain roughness heights k_s were calculated for each measured surface topography using the functional form from Forooghi *et al.* (2017), but reformulated in terms of k_{rms} and fitted to an expanded training data set by 'Aliman *et al.* (2026). These showed k_s values ranging from 0.3 to 2.0 mm along the line upstream of the LDA measurement window. Using a power-mean approach from Hutchins *et al.* (2023), a hull-averaged equivalent sand-grain roughness height $\overline{k_s} = 0.68$ mm and skin friction drag penalty $\Delta\overline{C_f} = 60.9\%$, were calculated. These were found to be very close to estimates based on the flow measurements; $\overline{k_s} = 0.56$ mm and $\Delta\overline{C_f} = 55.9\%$, respectively. This ability to predict the skin friction drag penalty directly from hull inspection is encouraging, suggesting that this methodology, coupled with hull scanning using the AQUAMARS platform, could prescribe an accurate cost to biofouling induced hull roughness, paving the way for more efficient management of the hull state across the fleet. Future work will focus on the further validation of this methodology; testing more roughness conditions as the hull of the test vessel continues to recruit fouling.

REFERENCES

'Aliman, I., Will, J. B., Nugroho, B., Monty, J. P. & Hutchins, N. 2026 Assessment and improvement of predictive models for estimating ship drag penalties from calcareous biofouling roughness. In *14th International Symposium on Turbulence and Shear Flow Phenomena, TSFP 2026*.

Chauhan, K. A., Nagib, h. & Monkewitz, P. 2007 On the composite logarithmic profile in zero pressure gradient turbulent boundary layers. In *45th AIAA Aerospace Sciences Meeting and Exhibit, Reno, NV*, , vol. 1, pp. 532–549.

European Maritime Safety Agency 2021 Facts and figures: The European maritime transport environmental report. *Tech. Rep.*. European Environment Agency.

Forooghi, P., Stroh, A., Magagnato, F., Jakirlić, S. & Frohnapfel, B. 2017 Toward a universal roughness correlation. *J. Fluids Eng.* **139** (12), 121201.

Granville, P. S. 1958 The frictional resistance and turbulent boundary layer of rough surfaces. *J. Ship res.* **2** (04), 52–74.

Hutchins, N., Ganapathisubramani, B., Schultz, M. P. & Pullin, D. I. 2023 Defining an equivalent homogeneous roughness length for turbulent boundary layers developing over patchy or heterogeneous surfaces. *Ocean Eng.* **271**, 113454.

Kempf, G. 1937 On the effect of roughness on the resistance of ships. *Trans INA* **79**, 109–119.

Kevin, K., Kogios, A., Will, J., Tsigaras, L., Monty, J. & Hutchins, N. 2025 AQUAMARS: An Operational Support System for Quantifying the Hydrodynamic Effects from Hull Roughness. In *Proc. Int. Mar. Conf.*.

Kodama, Y., Kakugawa, A., Takahashi, T. & Kawashima, H. 2000 Experimental study on microbubbles and their applicability to ships for skin friction reduction. *Int. J. Heat Fluid Flow* **21** (5), 582–588.

Monty, J. P., Allen, J. J., Lien, K. & Chong, M. S. 2011 Modification of the large-scale features of high Reynolds number wall turbulence by passive surface obtrusions. *Exp. Fluids* **51** (6), 1755–1763.

Monty, J. P., Dogan, E., Hanson, R., Scardino, A. J., Ganapathisubramani, B. & Hutchins, N. 2016 An assessment of the ship drag penalty arising from light calcareous tubeworm fouling. *Biofouling* **32** (4), 451–464.

Prandtl, L. & Schlichting, H. 1934 Das widerstandsgesetz rauher Platten. *Werft, Reederei, Hafen* **15** (1), 1–4.

Schultz, M. P., Bendick, J. A., Holm, E. R. & Hertel, W. M. 2011 Economic impact of biofouling on a naval surface ship. *Biofouling* **27** (1), 87–98.

Townsin, R. L. 2003 The ship hull fouling penalty. *Biofouling* **19** (S1), 9–15.

Vishwanathan, V., Hutchins, N. & Schultz, M. P. 2025 Evaluating the power mean method to determine an equivalent sandgrain roughness parameter over streamwise-heterogeneous roughness. *Flow* **5**, E23.

Woods Hole Oceanographic Institution 1952 Marine fouling and its prevention. *Tech. Rep.*. Navy Dept. Bureau of Ships, Annapolis, MD: US Naval Institute.